Dalton Transactions

ROYAL SOCIETY OF CHEMISTRY

PAPER

View Article Online
View Journal | View Issue

Check for updates

Cite this: *Dalton Trans.*, 2025, **54**, 2645

Low-coordinate bis-phosphine and monophosphine Ni(0) complexes: synthesis and reactivity in C–S cross-coupling†

M. Trinidad Martín,[a] Carlos J. Carrasco,[a] Nazaret Santamaría,[a] Celia Maya,[b] Auxiliadora Prieto,*[a] Agustín Galindo *[a] and M. Carmen Nicasio *[a]

Received 4th December 2024,
Accepted 2nd January 2025

DOI: 10.1039/d4dt03375b

rsc.li/dalton

Preformed Ni(0) complexes are rarely used as precatalysts in cross-coupling reactions, although they can incorporate catalytically active nickel directly into the reaction. In this work, we focus on the preparation and the catalytic application of low-coordinate Ni(0) complexes supported by bulky monophosphine ligands in C–S cross-coupling reactions. We have prepared two families of Ni(0) complexes, bis-phosphine aducts of the type [Ni(PR_2Ar')$_2$] (Ar′ = *m*-terphenyl group) and monophosphine derivatives of the type [Ni(PR_2Ar')(DVDS)] (DVDS = divinyltetramethyldisiloxane). DFT calculations were used to account for the atypical bent structures displayed by the bis-phosphine Ni(0) complexes. Monophosphine-Ni(0) complexes display catalytic activity superior to bis-phosphine Ni(0) adducts, which suggests that the former facilitate the generation of highly reactive monoligated PNi(0) species. Furthermore, the reactivity of monophosphine-Ni(0) precatalysts outperform that observed with Ni(II) precatalysts with the same phosphine ligands, supporting a more facile activation step to the same catalytic species. This enhanced reactivity allows for the use of lower catalyst loadings (1–5 mol%) and for carrying out the challenging coupling between aryl chlorides and alkylthiols.

Introduction

The quest for more sustainable solutions to precious metal catalysis has increased interest in processes catalyzed by first row transition metals, such as nickel.[1] In organic reactions catalyzed by nickel, low-coordinate Ni(0) species are often postulated as key intermediates.[1c,2] These reactive species are usually generated *in situ*, either by reduction of a Ni(II) precursor with an external reductant in the presence of the ligand,[3,4] or by reaction of Ni(COD)$_2$ (COD = 1,5-cyclooctadiene), the most often used Ni(0) source,[5] with the ligand. Although this method is operationally convenient, inefficient reduction and/or formation of species with a different metal–ligand ratio can negatively affect the reaction outcome.[1c,6] An alternative approach is to use a preformed Ni(0) complex, in which the ligand is coordinated to the metal, as a precatalyst. The group of Montgomery has successfully applied this strategy in Ni-catalyzed cycloaddition and C–H functionalization reactions.[6b,7] However, despite the advantage of not needing activation to enter the catalytic cycle, the use of single-component Ni(0) precatalysts in cross-coupling chemistry is uncommon.[8] Among Ni-catalyzed cross-coupling reactions, those involving the formation of C–S bonds have received less attention.[9] Most described catalyst systems rely on the use of supporting chelating ligands. These ligands are less susceptible to being displaced by nucleophilic thiolate anions, preventing catalyst deactivation.[10] With the exception of NHC-ligated Ni complexes, which demonstrated their catalytic competence in C–S cross-coupling,[11] we noted the absence of protocols based on Ni with non-chelating ancillary ligands such as monophosphines.[12] Building on our previous experience on Ni-catalyzed C–S bond formation,[11b] we developed[13] a family of Ni(II) precatalysts of the type [Ni(allyl)Cl(PMe_2Ar')]. These complexes effectively catalyzed the coupling of aromatic and aliphatic thiols with different electrophiles, including aryl tosylates for the first time (Scheme 1A). However, the C–S couplings with aryl chlorides required high catalyst loadings (10 mol%), and proceeded mainly with aromatic thiols. We envisaged that the use of preformed Ni(0) precatalysts could

[a]*Departamento de Química Inorgánica, Universidad de Sevilla, 41012 Sevilla, Spain. E-mail: mnicasio@us.es*
[b]*Instituto de Investigaciones Químicas (IIQ), Departamento de Química Inorgánica and Centro de Innovación en Química Avanzada (ORFEO-CINQA), Consejo Superior de Investigaciones Científicas (CSIC) and Universidad de Sevilla, Avenida Américo Vespucio 49, 41092 Sevilla, Spain*

†Electronic supplementary information (ESI) available: Experimental and computational details, spectroscopic and analytical data, X-ray crystallographic and computational data. CCDC 2405003 for **4**, 2405002 for **5**, 2405004 for **6**. For ESI and crystallographic data in CIF or other electronic format see DOI: https://doi.org/10.1039/d4dt03375b

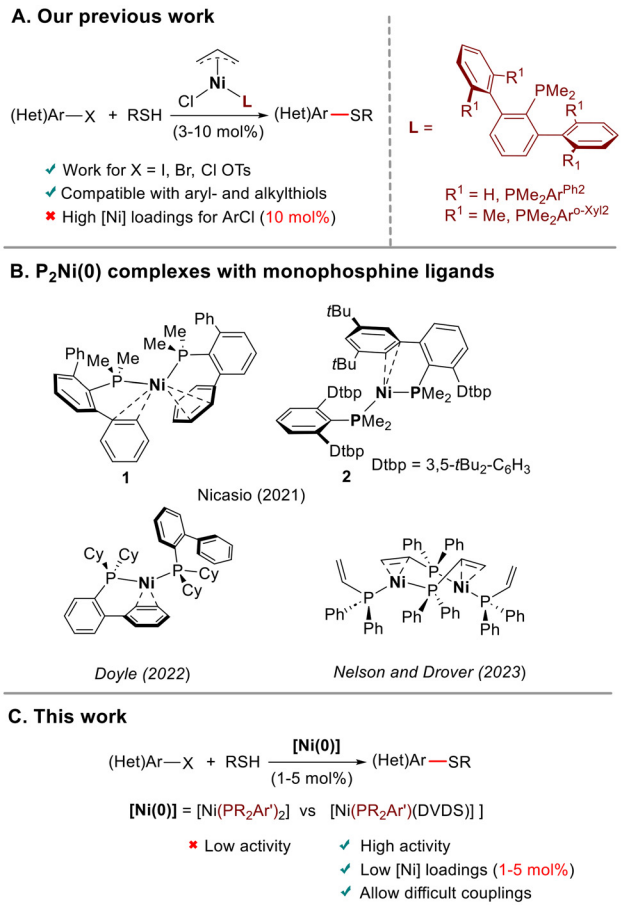

Scheme 1 (A) Our previous work on C–S cross-coupling using pre-formed Ni(II)-allyl precatalysts with terphenyl phosphine ligands. (B) $P_2Ni(0)$ complexes with monophosphine ligands. (c) This work.

facilitate these challenging transformations. In this regard, Doyle and co-workers[14] have demonstrated that monoligated PNi(0) accelerates oxidative addition and transmetallation steps, while bis-ligated $P_2Ni(0)$ species prevent catalyst deactivation.

Bis-ligated $P_2Ni(0)$ complexes with monophosphine ligands are rare.[15] We recently[16] isolated and structurally characterized two $P_2Ni(0)$ supported by terphenyl phosphines, which displayed bent structures (Scheme 1B). Shortly thereafter, the group of Doyle[17a] described the preparation of analogous $P_2Ni(0)$ derivatives using Buchwald biaryl phosphines and Nelson and Drover[17b] reported the preparation of dimeric species supported with allyl- and vinyldiphenylphosphines (Scheme 1B). To further explore the reactivity of these unusual low-coordinate $P_2Ni(0)$ species,[18] here we describe the synthesis and characterization of two new $P_2Ni(0)$ complexes supported by the ligands $PMe_2Ar^{m\text{-}Xyl2}$ ($Ar^{m\text{-}Xyl2}$ = 2,6-bis-(3,5-Me_2-C_6H_3)-C_6H_3) and $P(OPh)_2Ar^{Ph2}$ (Ar^{Ph2} = 2,6-Ph_2-C_6H_3), which exhibit bent P–Ni–P structures. We have analyzed the reasons that favor the bending in $P_2Ni(0)$ complexes using DFT calculations. Furthermore, we have prepared [Ni(PR_2Ar')(DVDS)] complexes by displacement of one of the phosphines in $P_2Ni(0)$ complexes with the diolefin ligand divinyltetramethyldisiloxane, DVDS. The latter could serve as synthons of monoligated PNi(0) species by diene extrusion. The behavior of both types of Ni(0) complexes as precatalysts in C–S cross-coupling has been examined. This study highlights the superior reactivity of monophosphine-ligated complexes, which outperform the results obtained with our terphenyl phosphine-supported Ni(II)-allyl precatalysts (Scheme 1C).

Results and discussion

Synthesis and characterization of [Ni(PR_2Ar')$_2$] and [Ni(PR_2Ar')(DVDS)]

As we described earlier,[16] we succeeded in preparing the bis-phosphine complex [Ni(PMe_2Ar^{Ph2})$_2$] **1**, in good yields, by the reaction of Ni(COD)$_2$ with 2 equiv. of the less bulky terphenyl phosphine PMe_2Ar^{Ph2} (Ar^{Ph2} = 2,6-$Ph_2C_6H_3$) in THF at room temperature. However, when increasing the steric bulk of the terphenyl moiety, by placing *t*Bu groups at *meta* positions of the flanking phenyl rings, no displacement of COD ligand occurred, albeit the complex [Ni(PMe_2Ar^{Dtbp2})$_2$] **2**, (Ar^{Dtbp} = 2,6-(3,5-*t*$Bu_2C_6H_3$)$_2C_6H_3$) could be prepared in moderate yield by heating the reaction under hydrogen pressure.[16]

We further expanded the family $P_2Ni(0)$ complexes by reacting Ni(COD)$_2$ with the ligands $PMe_2Ar^{m\text{-}Xyl2}$ ($Ar^{m\text{-}Xyl2}$ = 2,6-(3,5-$Me_2C_6H_3$)$_2C_6H_3$) and $P(OPh)_2Ar^{Ph2}$. Compounds **3** and **4** were obtained as air-sensitive reddish solids in good yields from the direct displacement of COD by the corresponding P-based ligand (Scheme 2A). However, terphenyl phosphines with *ortho*-substitution on the flanking rings or with P-bound substituents larger than methyl failed to produce any products by this synthetic route. We then focused on synthetic strategies that avoid the use of Ni(COD)$_2$ as the metal precursor. We found that complex **2** could be obtained with high yields by reducing Ni(acac)$_2$ with $AlMe_3$ in the presence of 2 equiv. of PMe_2Ar^{Dtbp2} (Scheme 2B). Using this strategy, we could observe, by ^{31}P NMR, the formation of the complex [Ni($PMe_2Ar^{o\text{-}Xyl2}$)$_2$], bearing the phosphine ligand with *ortho* substitution on the flanking rings of the terphenyl moiety. However, the instability of this species in solution prevented its isolation and full characterization.

The new complexes **3** and **4** displayed NMR features similar to those described for adducts **1** and **2**. Room temperature $^{31}P\{^1H\}$ NMR spectra of **3** and **4** in C_6D_6 show the equivalence of both phosphorus ligands, as indicated by the presence of sharp singlets at −0.5 and 160.4 ppm, respectively. Additionally, the ^1H and $^{13}C\{^1H\}$ NMR spectra of **3** clearly show the presence of a virtual coupled triplet for the methyl groups bonded to the phosphorus nuclei.

The molecular structure of **4**, determined by X-ray diffraction studies (Scheme 2C) is very similar to that of **1**, with the two phosphine ligands adopting pseudobidentate modes, κ^1-P,η^2-C_{arene}. Both Ni–C_{arene} interactions were of different magnitude. The shortest separations occurred between Ni–C_{ortho}(C1) (2.086(2) Å) and Ni–C_{meta}(C2) (2.211(2) Å) of a flanking phenyl

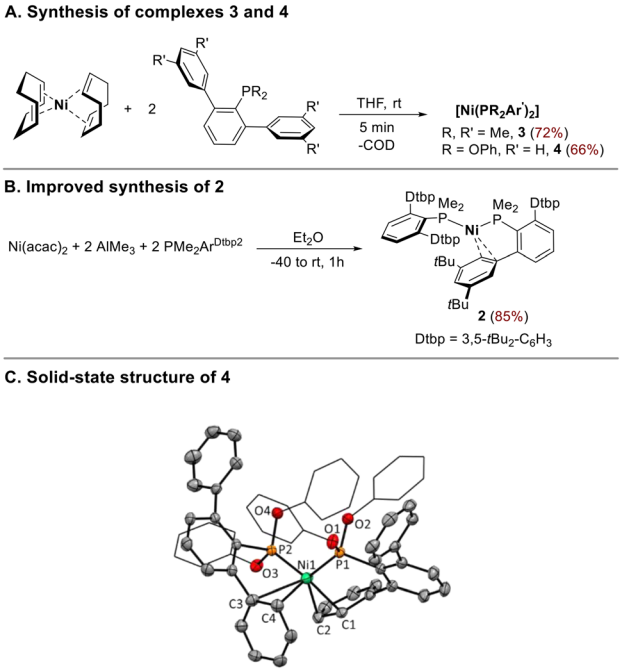

Scheme 2 (A) Synthesis of NiP_2 complexes **3** and **4**. (B) Improved synthetic route for $[Ni(PMe_2Ar^{Dtbp2})_2]$, **2**. (C) Molecular structure of **4**. Hydrogen atoms are omitted for the sake of clarity. Thermal ellipsoids are shown at a 50% probability. Selected bond lengths [Å] and angles [°]: Ni–P1 2.1253(5), Ni–P2 2.1074(5), Ni–C1 2.086(2), Ni–C2 2.211(2), Ni–C3 2.614(2), Ni–C4, 2.4261(2), P1–Ni–P2 115.37(2).

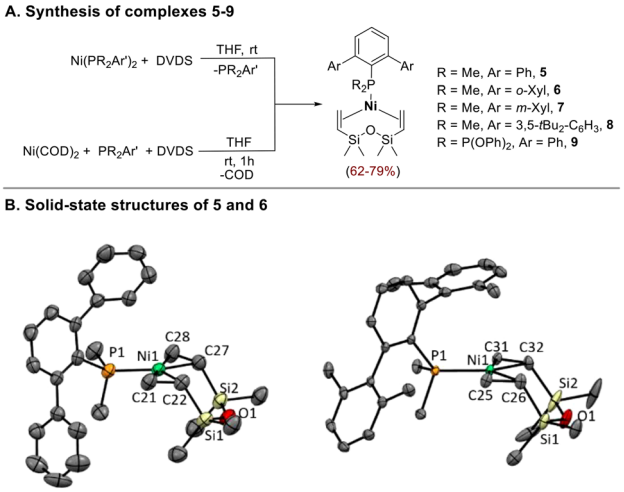

Scheme 3 (A) Synthesis of $[Ni(PR_2Ar')(DVDS)]$ complexes **5–9**. (B) Molecular structures of **5** (left) and **6** (right). Hydrogen atoms are omitted for the sake of clarity. Thermal ellipsoids are shown at a 50% probability. Selected bond lengths [Å] and angles [°] for **5**: Ni1–P1 2.162 (1), Ni1–C21 1.986(4), Ni1–C22 2.000(4), Ni1–C27 2.019(3), Ni1–C28 1.995(3), C21–C22 1.398(6), C27–C28 1.293(5), P1–Ni1–C21 92.1(1), P1–Ni1–C22 132.4(1), P1–Ni–C27 133.1(1), P1–Ni1–C28 93.2(1); for **6**: Ni1–P1 2.1669(8), Ni1–C25 1.998(2), Ni1–C26 2.008(2), Ni1–C31 2.017(2), Ni1–C32 1.990(2), C25–C26 1.411(4), C31–C32 1.406(3), P1–Ni1–C25 91.67(8), P1–Ni1–C26 132.58(8), P1–Ni–C31 133.74(7), P1–Ni1–C32 92.70(7).

ring of one of the phosphine ligands. The other Ni–C_{arene} interaction was much less pronounced and involved the C_{ipso}(C3) and C_{ortho}(C4) of a side ring of the second phosphine, with distances ranging from 2.461(2) to 2.614(2) Å, much longer to those found in the phosphine adduct **1** (2.322(3) and 2.403(3) Å).[16] Overall, the shortest Ni–C_{arene} distances and the P–Ni–P angle (115.37(2) °) were comparable to those found in **1** and in biaryl phosphine analogues.[17a] Finally, the slightly shorter Ni–P bond distances (2.1074(5) and 2.1253(5) Å) compared to those in **1** (average 2.18 Å) reflected the π-acceptor character of the phosphonite ligand.

One of the phosphorous ligands in $P_2Ni(0)$ complexes **1–4** can be easily replaced by the chelating olefin DVDS at room temperature,[19] giving the coordinatively unsaturated monophosphine species **5–9** (Scheme 3). Alternatively, these compounds are directly prepared by the reaction of $Ni(COD)_2$ with DVDS (2 equiv.) in the presence of the appropriate terphenyl phosphine at room temperature (Scheme 3). All compounds except **8** were isolated as yellow crystalline solids by addition of pentane to the reaction mixtures. Complex **8** defied all efforts at isolation due to its thermal sensitivity, but its formation could be confirmed by NMR analysis of the reaction mixtures in C_6D_6 (see ESI† for details).

The ^{1}H NMR spectra of **5–9** show two signals for the methyl groups on the silicon atoms of the DVDS ligand and two resonances between 2–3 ppm assigned to the vinyl protons.[3,19] Due to unhindered rotation of the phosphine ligand around the Ni–P bond, the PMe_2 groups give rise to a doublet and the substituents on the flanking rings of the terphenyl moiety (*i.e.* Me or *t*Bu) originate a single resonance, both in the ^{1}H and $^{13}C\{^1H\}$ NMR spectra.

Crystals suitable for X-ray diffraction studies of **5** and **6** were obtained by slow recrystallization from petroleum ether/THF mixtures at −20 °C. The structures shown in Scheme 3B are rare examples of crystallographically characterized monophosphine-supported Ni(0) species with DVDS ligand.[3,20] In both structures the Ni atom lies in a planar trigonal environment formed by the P atom and the two vinyl groups of the DVDS ligand. The six-membered metallacycle rings adopt a chair conformation. The Ni–P bond lengths (2.162(1) Å in **5** and 2.1669(8) in **6**) are slightly shorter than those reported for the related complexes $[Ni(PCy_3)(DVDS)]$[20] (2.2060(9) Å) and $[Ni(PtBuiPr_2)(DVDS)]$[3] (2.2284(10) Å). The elongated C=C bond distances in the coordinated diene molecule, mean value of 1.40 Å for **5** and 1.41 Å for **6**, falls within the range reported for Ni(0)-DVDS complexes bearing σ-donor ligands[3,20,21] and proves the metal backdonation.

Computational studies

NiP_2 complexes with terphenyl phosphines **1–2**[16] and terphenyl phosphonite **4** as well as those supported by biaryl phosphines[17a] display uncommon bent structures for d^{10}-ML_2 complexes.[22] Bickelhaupt and coworkers[23] have found that the bending of the angle L–M–L in d^{10}-ML_2 complexes is a consequence of π-backbonding. When π backbonding is strong, a lower

L-M–L angle favors the donor–acceptor orbital interaction with a high-energy donor orbital of the metal fragment, producing an additional stabilization.[23b] Furthermore, bent ML_2 fragments are found when d^{10}-ML_2 complexes react with additional π-acid ligands forming triangular planar 16-electron d^{10}-ML_3 structures. This is a consequence of the topology of the bent d^{10}-ML_2 HOMO, which is made up of a polarized dp orbital specifically suited for a π-backdonation to the extra ligand. Indeed, this is the situation encountered for complexes **1–4** and for $P_2Ni(0)$ complexes containing biaryl phosphine ligands.[17a]

However, we questioned why bent P–M–P structures occurred for nickel derivatives, whereas $P_2M(0)$ complexes of its heavier counterparts, Pd and Pt with terphenyl phosphines, displayed linear geometry.[16] To gain information about the reasons behind such different behavior, we carried out computational studies using the complexes $[M(C_2H_4)(PMe_2Ph)_2]$ (M = Ni, Pd, Pt) as the model systems (see ESI, Fig. S1†). We calculated the energies of the reaction between $[M(PMe_2Ph)_2]$ complexes and ethylene (ESI, Table S1†). In this reaction, there are two opposing effects: the stabilization produced by the ethylene coordination and the destabilization caused by the P–M–P bending. Interestingly, the process turned out to be exergonic for the nickel complex (ΔG = −10.6 kcal mol^{-1}), while for the Pd and Pt derivatives the reactions were unfavorable (ΔG = 5.6 and 7.6 kcal mol^{-1}, respectively). These findings suggest that additional coordination of an extra ligand counterbalances the P–M–P bending only if the metal is nickel, in good agreement with the experimental observations and with the results obtained by Bickelhaupt and Radius for related d^{10}-$[M(NHC)_2]$ complexes of group 10 metals.[23c]

Geometry optimizations were performed for $[Ni(PMe_2Ar^{Ph2})_2]$, **1**, $[Ni(PMe_2Ar^{Dtbp2})_2]$, **2**, $[Ni(PMe_2Ar^{m\text{-}Xyl2})_2]$, **3**, and $[Ni(P(OPh)_2Ar^{Ph2})_2]$, **4** (ESI, Fig. S2†). They showed pseudo-tetrahedral geometries that compared well with the experimental ones for **1**, **2** and **4**. However, we found some discrepancies between the computed and experimental Ni–C_{arene} distances with the flanking phenyl rings (ESI, Table S2†). In these structures, the Ni–C_{arene} separations with the closer phenyl ring were well described by calculations, while for the furthest one the optimized Ni–C_{arene} distances were above 3 Å. Although such inconsistencies can be ascribed to the difference between experimental solid-state and gas-phase calculated structures, they also seem to point to the lability of these Ni–C_{arene} interactions. In fact, NMR spectra of complexes **1–4** show the equivalence of the two phosphorus ligands. Since variable temperature NMR experiments carried out with complex **1**[16] did not provide any information about the dynamic process that occurs in solution (ESI, Fig. S3†), we studied the dynamic behavior of **1** by DFT calculations (see Scheme 4). It is triggered by the temporary cleavage of one of the weak Ni–η^2-C_{arene} bonds. Then, the second η^2-Ph ring is detached from the metal center with a concomitant loss of the bent disposition towards a lineal arrangement. The ΔG energy difference between the pseudo-tetrahedral structure and the lineal structure in toluene is 9.9 kcal mol^{-1}, in agreement with the observed fluxionality.

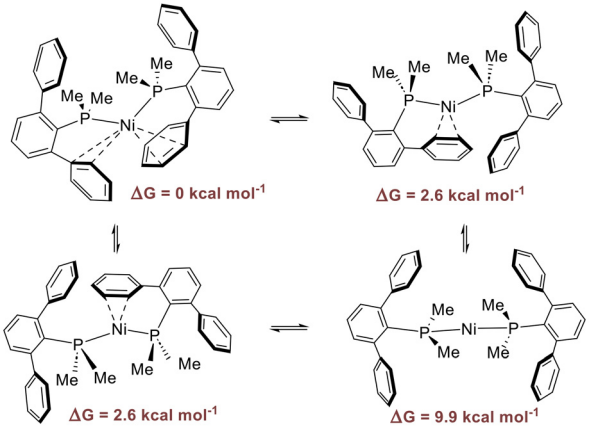

Scheme 4 Dynamic process that averages the phosphine environment in solution.

Geometry optimizations were also performed for divinyldisiloxane complexes **5–9** (ESI, Fig. S3†). They showed the typical trigonal-planar structure of the d^{10}-ML_3 complexes. A good comparison of the calculated structural parameters with the experimental ones was observed for **5** and **6**, except for the Ni–P bond distance, which is slightly overestimated (ESI, Table S3†). The HOMO to HOMO−4 orbitals are the five d orbitals, as expected for a d^{10}-ML_3 complex (Fig. S4† for complex **5**). In particular, HOMO to HOMO−2 are basically pure d orbitals (HOMO, z^2; HOMO−1, yz; and HOMO−2, xz), while backdonations to vinyl groups come from HOMO−3 (xy) and HOMO−4 ($x^2 - y^2$). The thermodynamics of the two synthetic pathways for the synthesis of complexes **5–9**, namely, starting from $P_2Ni(0)$ and from $Ni(COD)_2$ (Scheme 3A), were analyzed. All reactions were exergonic (ESI, Table S4†) in agreement with experimental. For this purpose, the complex $[Ni(PMe_2Ar^{o\text{-}Xyl2})_2]$, not experimentally isolated, was also optimized (ESI, Fig. S2 and Table S2†). This complex is 18.2 kcal mol^{-1} less stable (electronic energy) than $[Ni(PMe_2Ar^{m\text{-}Xyl2})_2]$, **3**, probably due to the steric pressure of *ortho* methyl substituents that prevents the stabilization of one of the flanking aryl groups (Fig. S2†).

Catalytic studies

Since both $P_2Ni(0)$ and $PNi(0)$ could serve as on-cycle species in C–S cross-couplings,[10,12] we sought to examine the catalytic performance of bis-phosphine and monophosphine Ni(0) precatalysts and C–S coupling reactions. To investigate the performance of terphenyl phosphines Ni(0) complexes **1–9**, we selected the coupling of iodobenzene with thiophenol in the presence of NaO*t*Bu as the model system (Table 1). Initially, we applied the optimized conditions found for the Ni(II)-allyl precatalysts.[13] All NiP_2 precatalysts **1–4** were active, but none of them provided full conversions even at extending the reaction time (Table 1, entries 1–4). Under these conditions, complex **2**, which contains the ligand PMe_2Ar^{Dtbp2}, displayed the higher catalytic activity. This could suggest a more facile dissociation of one of the phosphine ligands in complex **2**, leading to reac-

Table 1 Evaluation of the catalytic activity of bis-phosphine and mono-phosphine Ni(0) complexes in the cross-coupling reaction between iodobenzene and thiophenol[a]

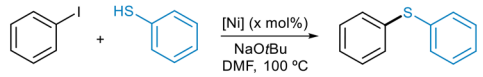

	Entry	[Ni] (mol%)	Time/h	Conv.[b]/%
NiP_2	1	**1** (3)	24	21
	2	**2** (3)	24	45
	3	**3** (3)	24	11
	4	**4** (3)	24	5
	5	**1** (10)	24	100 (93)[c]
	6	**2** (10)	24	(80)[c]
NiP(DVDS)	7	**5** (3)	6	100
	8	**5** (1)	6	99
	9	**5** (0.5)	6	51
	10	**5** (1)	4	100 (93)[c]
	11	**6** (1)	4	97 (95)[c]
	12	**7** (1)	4	77
	13	**9** (1)	4	41

[a] Reaction conditions: iodobenzene (1.0 mmol), thiophenol (1.1 mmol), NaO*t*Bu (1.2 mmol), DMF (1 mL), T = 100 °C. [b] Conversion determined by GC using dodecane as internal standard (average of two runs). [c] Isolated yield of the product.

tive monoligated PNi(0) species. In fact, the largest difference between the two Ni–P bond lengths among the NiP_2 series was found in the solid state structure of **2** (see Table S2 in ESI† for bond metrics comparisons). We only observed high yields with precatalysts **1** and **2** when using 10 mol% catalyst loadings (entries 5 and 6; see also Table S5 in ESI† for further reaction conditions). Unlike the bis-phosphine complexes, monophosphine NiP(DVDS) derivatives were much more reactive. Therefore, compound **5** provided complete conversions under the best conditions applied for the Ni-allyl precatalysts (Table 1, entry 7). We selected **5** for reoptimization of the reaction parameters (see ESI, Table S5†). We found that by reducing the catalyst loading to 1 mol% and the reaction time to 4 h, the diphenyl sulfide product was produced in quantitative yields (Table 1, entries 8–10). Under the optimized conditions, only precatalyst **6** led to full conversions (entries 11–13). Unfortunately, the thermal instability of **8** prevented us from studying its reactivity in these coupling reactions. Finally, we tested the most active precatalysts **5** and **6** in the coupling of bromobenzene and phenyl tosylate with thiophenol (Table 2 and Table S6 in ESI†). For both electrophiles, quantitative yields were achieved at lower Ni loadings (3 mol%) and shorter reaction times (4 h) than those required for the monophosphine Ni(II)-allyl precatalysts. Overall, these results confirmed that the terphenyl phosphines PMe_2Ar^{Ph2} and $PMe_2Ar^{o\text{-}Xyl2}$ were the best performing ligands in these C–S couplings.[13] Furthermore, they highlighted the remarkable catalytic activity of complexes **5** and **6**, which outperformed that of our Ni(II)-allyl precatalysts. These results point towards a more facile rate of activation of preformed monoligated PNi(0) complexes to catalytically active species.

Table 2 Screening of precatalysts **5** and **6** in the coupling of thiophenol with bromobenzene and phenyl tosylate[a]

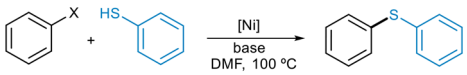

Entry	X	[Ni] (mol%)	Time/h	Conv.[b]/%
1[c]	Br	**5** (5)	6	100
2	Br	**5** (3)	4	99 (92)[d]
3	Br	**6** (3)	4	94 (91)[d]
4[e]	OTs	**5** (5)	6	100
5	OTs	**5** (3)	4	92 (79)[d]
6	OTs	**6** (3)	4	88 (77)[d]

[a] Reaction conditions: aryl halide (1.0 mmol), thiophenol (1.1 mmol), base (1.2 mmol), DMF (1 mL) T = 100 °C. [b] Conversion determined by GC using dodecane as internal standard (average of two runs). [c] Optimized conditions found for the coupling of bromobenzene with thiophenol catalyzed by Ni(II)-allyl using NaO*t*Bu as the base (see ref. 13). [d] Isolated yield of the product. [e] Optimized conditions found for the coupling of bromobenzene with thiophenol catalyzed by Ni(II)-allyl using LiO*t*Bu as the base (see ref. 13).

We explored the scope of C–S cross-coupling with a small array of aryl iodides, bromides, and tosylates using the most active precatalysts **5** and **6**. All cross-coupled products were obtained in useful synthetic yields under the optimized reaction conditions (Scheme 5). Both catalyst systems were very active in reactions involving sterically hindered substrates, providing the products in high yields (**10c** and **10d**).

Furthermore, C–I, C–Br or C–OTs bonds were selectively functionalized in the presence of a chloride or a fluoride functionality (**10e** and **10f**). Similarly, free –SH group was efficiently

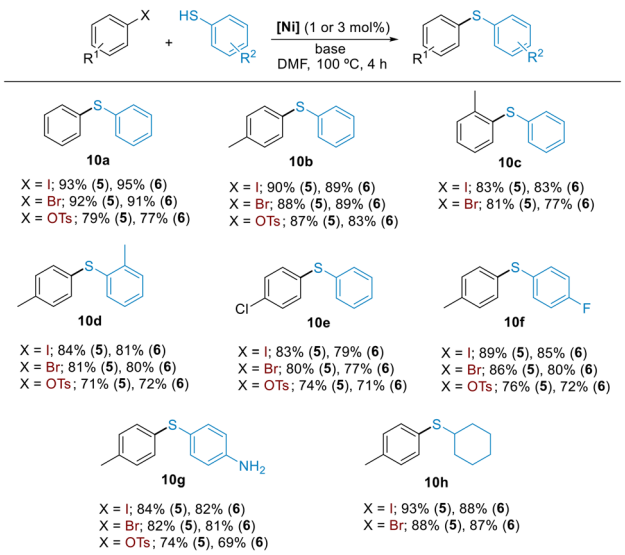

Scheme 5 Scope of the arylation of thiols with aryl iodides, bromides and tosylates catalyzed by **5** and **6**. Reaction conditions: aryl halide (1.0 mmol), thiol (1.1 mmol), base (NaO*t*Bu for X = I, Br, and LiO*t*Bu for X = OTs; 1.2 mmol), **5** or **6** (1 mol% for reactions with aryl iodides and 3 mol% for reactions with aryl bromides and tosylates), DMF (1 mL), 100 °C, 4 h. Isolated yields of pure products (average of two experiments).

arylated in the presence of a competing protic functionality (**10g**). Furthermore, aliphatic thiols were also compatible substrates and cyclohexanethiol was successfully arylated using the protocol developed (**10h**).

Given that aryl chlorides were the least reactive substrates in our previous protocol with Ni(II)-allyl precatalysts,[13] we sought to determine whether monophosphine Ni(0) precatalysts could facilitate the activation of challenging C–Cl bonds. The catalytic study was carried out with complex **5** as a precatalyst. Gratifyingly, the coupling of chlorotoluene with thiophenol proceeded in quantitative yields applying the reaction conditions found for the Ni(II)-allyl precatalysts, but with half the catalyst loading (Table 3, entry 1). Further reduction of the catalyst loading led to lower conversions (entries 2 and 3).

Encouraged by this result, we targeted more challenging couplings, such as the thioetherification of aliphatic thiols with chloroarenes. Reports on this type of C–S couplings employing Ni catalyst remain rare.[24] Under the optimized conditions shown in Table 3, we examined the coupling of (hetero)aryl chlorides with alkylthiols (Scheme 6). Electron-rich and electron-poor aryl chlorides as well as 2-chloropyridine reacted with primary (**11a–11c**), secondary (**11d–11f**) and tertiary (**11g–11h**) alkyl thiols in good isolated yields. The reaction of hindered 2-chloro-toluene occurred to form the product **11i**, but with moderate yield. These results highlight the high reactivity of precatalyst **5** in the C–S cross-coupling of both aromatic and aliphatic thiols, significantly improving the results we obtained with Ni(II)-allyl precatalysts.[13] Additionally, this study demonstrates the effective steric protection imparted by the terphenyl phosphine ligand to the Ni center, preventing the catalyst deactivation by binding of multiple thiolate ligands.

Table 3 Optimization of reaction conditions for the C–S coupling of chlorobenzene with thiophenol catalyzed by **5**[a]

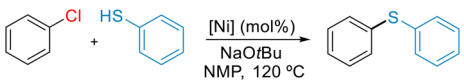

Entry	[Ni] (mol%)	Yield[b]/%
1	**5** (5)	95
2	**5** (2.5)	79
3	**5** (1)	65

[a] Reaction conditions: chlorobenzene (0.55 mmol), thiophenol (0.5 mmol), base (0.6 mmol), NMP (0.5 mL) T = 120 °C, time = 16 h (not optimized). [b] Isolated product yield (average of two runs).

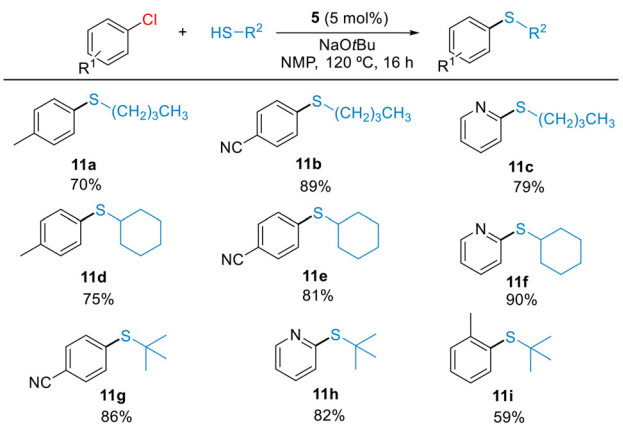

Scheme 6 Scope of alkylthiols arylations with aryl chlorides catalyzed by **5**. Reaction conditions: aryl chloride (0.55 mmol), thiol (0.5 mmol), NaO*t*Bu (0.6 mmol), **5** (5 mol%), NMP (0.5 mL), 120 °C, 16 h (not optimized). Isolated yields of pure products (average of two experiments).

Conclusions

We have synthesized and structurally characterized two bis-phosphine Ni(0) complexes of the type [Ni(PR_2Ar')$_2$], supported by bulky terphenyl phosphine ligands. The compounds are fluxional in solution, and X-ray diffraction study demonstrates that they are not truly 14-electron species but rather 16-electron species in which one of the phosphorus ligands is bonded in pseudobidentate fashion (k^1-P, Ni–C_{arene}). DFT calculations provide an explanation for the preferred bending structures displayed by these d^{10}-ML_2 complexes. These studies show that the coordination of the Ni center to one double bond of a side ring of the terphenyl moiety counterbalances the destabilization effect of the P–M–P bending. This Ni–η^2-C_{arene} bond is weak and the stepwise dissociation of such an interaction theoretically justifies the dynamic NMR spectra of **1–4**.

The displacement of one of the phosphorus ligands in P_2Ni(0) complexes by diene DVDS is facile, allowing the preparation of a series of monophosphine Ni(0) complexes of the type [Ni(PR_2Ar')(DVDS)]. These complexes can also be synthesized directly from Ni(COD)$_2$. Both synthetic processes are exergonic according to DFT calculations.

Bis-phosphines and monophosphine Ni(0) complexes have been tested as precatalysts in C–S bond formation reactions with the latter showing the best catalytic performance. Among all Ni-DVDS compounds tested, those supported by the parent terphenyl phosphine PMe_2Ar^{Ph2}, **5**, or by the phosphine $PMe_2Ar^{o\text{-}Xyl2}$, **6**, are the most active precatalysts. These results suggest that monoligated PNi(0) could be the catalytically reactive intermediates and that monophosphine Ni(0) precatalysts provide a more facile formation of these highly unsaturated species. Moreover, the catalytic performance of **5** and **6** is also superior to that of Ni(II)-allyl precatalysts with the same phosphine ligands, which highlights the advantage of using preformed Ni(0) precatalysts to enhance rate of activation to PNi(0) catalytic species. The increased reactivity of **5** and **6** enables the performance of C–S couplings at lower catalyst loadings (1–5 mol%) and the successful achievement of the challenging thioetherification of aryl chlorides with alkylthiols. Finally, this study also provides some insight into the remarkable ability of terphenyl phosphines to stabilize highly unsaturated monoligated PNi(0) reactive species, preventing their deactivation in the presence of thiolate ligands.

Experimental

General considerations

All preparations and manipulations were performed under an oxygen-free nitrogen atmosphere using standard Schlenk techniques. The solvents were rigorously dried and degassed before use. Reagents were purchased from commercial suppliers and used without further purification. The dimethylterphenyl phosphines PMe_2Ar^{Ph2},[25] $PMe_2Ar^{m\text{-}Xyl2}$,[13] $PMe_2Ar^{o\text{-}Xyl2}$,[25] PMe_2Ar^{Dtbp2},[26] and $Ni(COD)_2$[27] were prepared according to procedures described. Solution NMR spectra were recorded on Bruker Avance III 300 MHz and Avance III 500 MHz spectrometers. The ^1H and ^{13}C resonances of the solvent were used as the internal standard and the chemical shifts are reported relative to TMS while ^{31}P was referenced to external H_3PO_4. Elemental analyses were performed by the Servicio de Microanálisis of the Instituto de Investigaciones Químicas (IIQ). X-ray diffraction studies were performed at Centro de Investigación, Tecnología e Innovación de la Universidad de Sevilla (CITIUS) and at the Instituto de Investigaciones Químicas (IIQ).

General procedure for the synthesis of $[Ni(PR_2Ar')_2]$ complexes 3 and 4

A solution of phosphine (0.2 mmol) in THF (1 mL) was added to a solution of $Ni(COD)_2$ (27.6 mg, 0.1 mmol) in THF (1 mL) under nitrogen. The resulting dark red solution was stirred for 5 minutes and petroleum ether was added to precipitate the corresponding complex. The title compound was obtained as dark red crystals after recrystallization.

General procedure for the synthesis of $[Ni(PR_2Ar')(DVDS)]$ complexes 5–9

To a solution of $Ni(COD)_2$ (44.3 mg, 0.16 mmol) in THF (2 mL), 1,3-divinyltetramethyldisiloxane (72 μL, 0.36 mmol) was added. The reaction was stirred for 5 minutes at room temperature, after which a solution of the ligand PR_2Ar (0.16 mmol) in THF (2 mL) was added. The mixture was stirred for 1 h and the product was precipitated by adding pentane. The solid was purified by recrystallization in a mixture of THF : petroleum ether (1 : 2).

Catalytic procedures for the C–S coupling of aryl iodides/bromides with aromatic/aliphatic thiols

The precatalysts **5** or **6** (0.01 or 0.03 mmol) and the base NaO*t*Bu (1.2 mmol) were dissolved in DMF or (1 mL) in a vial equipped with a J Young tap containing a magnetic bar. The thiol (1.1 mmol) and the aryl iodide/bromide/tosylate (1 mmol) were added in turn under a nitrogen atmosphere. The mixture was stirred at 100 °C for 4 h in an oil bath. The reaction mixture was cooled to room temperature, diluted with ethyl acetate (10 mL) and filtered through a Celite plug. The conversion was determined by GC analysis using dodecane as an internal standard. Pure products were obtained after purification by flash chromatography on silica gel with petroleum ether.

Computational details

The electronic structure and geometries of the compounds were investigated by using density functional theory (DFT) at the B3LYP level[28,29] using the 6-311G(d) basis set. Molecular geometries were optimized without symmetrical restrictions. Frequency calculations were carried out at the same level of theory to identify all stationary points as minima (zero imaginary frequencies) and to provide the thermal correction to the free energy at 298.15 K and 1 atm. The energies of the reaction between $[M(PMe_2Ph)_2]$ complexes and ethylene were calculated from the optimized reactants and products using the 6-311++G(d, p) basis set and LANL2DZ[30] for the Pd and Pt atoms. The energies of the fluxional behavior of complex **1** were calculated using single-point calculations with the 6-311++G(d,p) basis set. In this case, solution-phase SCF energies were calculated using the CPCM solvation model in toluene.[31] The DFT calculations were carried out using the Gaussian 09 program package.[32]

Author contributions

The manuscript was written through contribution of all authors. MTM, CJC and NS designed and conducted experiments and analyzed the data. CM conducted X-ray diffraction analysis. AG carried out the computational studies and contributed to the manuscript writing. MCN and AP conceptualized and supervised the project and drafted the script.

Data availability

All data supporting this article have been included as part of the ESI.†

Conflicts of interest

There are no conflicts to declare.

Acknowledgements

We thank financial support from MCIU/AEI/10.13039/501100011033 (Grant PID2020-113797RB-C22) and MCIU/AEI/10.13039/501100011033 and ERDF/EU (Grant PID2023-151417NB-100). The use of computational resources of the Universidad de Granada (cluster Albaicín) is thankfully acknowledged.

References

1 (*a*) S. Z. Tasker, E. A. Standley and T. F. Jamison, *Nature*, 2014, **509**, 299–309; (*b*) V. P. Ananikov, *ACS Catal.*, 2015, **5**, 1964–1971; (*c*) C. M. Lavoie and M. Stradiotto, *ACS Catal.*, 2018, **8**, 7228–7250; (*d*) *Nickel Catalysis in Organic Synthesis: Methods and Reactions*, ed. S. Ogoshi, Wiley-VCH,

Weinheim, Germany, 2020; (*e*) A. L. Clevenger, R. M. Stolley, J. Aderibigbe and J. Louie, *Chem. Rev.*, 2020, **120**, 6124–6196.

2 (*a*) N. I. Saper, A. Ohgi, D. W. Small, K. Semba, Y. Nakao and J. F. Hartwig, *Nat. Chem.*, 2020, **12**, 276–283; (*b*) J. B. Diccianni and T. Diao, *Trends Chem.*, 2019, **1**, 834–844; (*c*) S. Cañellas, J. Montgomery and M. À. Pericàs, *J. Am. Chem. Soc.*, 2018, **140**, 17349–17355; (*d*) S. Tang, O. Eisenstein, Y. Nakao and S. Sakaki, *Organometallics*, 2017, **36**, 2761–2777; (*e*) J. A. Garduño, A. Arévalo and J. J. García, *Dalton Trans.*, 2015, **44**, 13419–13438; (*f*) R. M. Stolley, H. A. Duong and J. Louie, *Organometallics*, 2013, **32**, 4952–4960.

3 (*a*) E. Richmond and J. Moran, *Synthesis*, 2018, 499–513; (*b*) E. Morser, J. Jeanneau, N. Mézailles, H. Olivier-Bourbigou and P.-A. R. Breuil, *Dalton Trans.*, 2019, **48**, 4101–4014.

4 An electrochemical method for the synthesis of Ni(0) complexes have been recently reported: C. Z. Rubel, Y. Cao, T. E.-H. Ewing, G. Laudadio, G. L. Beutner, S. R. Wisniewski, X. Wu, P. S. Baran, J. C. Vantourout and K. M. Engle, *Angew. Chem., Int. Ed.*, 2024, **63**, e202311557.

5 A variety of bench-stable Ni(0) precursors for in situ ligation protocols have been reported in recent years: (*a*) V. T. Tran, Z.-Q. Li, O. Apolinar, J. Derosa, M. V. Joannou, S. R. Wisniewski, M. D. Eastgate and K. M. Engle, *Angew. Chem., Int. Ed.*, 2020, **59**, 7409–7413; (*b*) L. Nattmann, R. Saeb, N. Nöthling and J. A. Cornella, *Nat. Catal.*, 2020, **3**, 6–13; (*c*) L. Nattmann and J. A. Cornella, *Organometallics*, 2020, **39**, 3295–3300; (*d*) C. Z. Rubel, W.-J. He, S. R. Wisniewski and K. M. Engle, *Acc. Chem. Res.*, 2024, **57**, 312–326.

6 (*a*) E. A. Standely and T. F. Jamison, *J. Am. Chem. Soc.*, 2013, **135**, 1585–1592; (*b*) A. J. Nett, J. Montgomery and P. M. Zimmerman, *ACS Catal.*, 2017, **7**, 7352–7362; (*c*) M. M. Beromi, G. Benerjee, G. W. Brudvig, D. J. Charboneau, N. Hazari, H. M. C. Lant and B. Q. Mercado, *Organometallics*, 2018, **37**, 3943–3955.

7 (*a*) A. J. Nett, W. Zhao, P. Zimmerman and J. Montgomery, *J. Am. Chem. Soc.*, 2015, **137**, 7636–7639; (*b*) A. J. Nett, S. Cañellas, Y. Higushi, M. T. Robo, J. M. Kochkodan, M. T. Haynes II, J. W. Kampf and J. Montgomery, *ACS Catal.*, 2018, **6**, 6606–6611; (*c*) M. T. Robo, A. R. Frank, E. Butler, A. J. Nett, S. Cañellas, P. Zimmerman and J. Montgomery, *Organometallics*, 2022, **41**, 3293–3300.

8 N. Hazari, P. R. Melvin and M. M. Beromi, *Nat. Rev. Chem.*, 2017, **1**, 0025.

9 (*a*) For recent reviews see: I. P. Beletskaya and V. P. Ananikov, *Chem. Rev.*, 2022, **122**, 16110–16293; (*b*) V. J. Geiger, R. M. Oechsner, P. H. Gehrtz and I. Fleischer, *Synthesis*, 2022, 5139–5167; (*c*) E. Rufino-Felipe, H. Valdés and D. Morales-Morales, *Eur. J. Org. Chem.*, 2022, e202200654.

10 (*a*) E. Alvaro and J. F. Hartwig, *J. Am. Chem. Soc.*, 2009, **131**, 7858–7868; (*b*) G. Yin, I. Kalvet, U. Englert and F. Schoenebeck, *J. Am. Chem. Soc.*, 2015, **137**, 4164–4172.

11 (*a*) Y. Zhang, K. C. Ngeow and J. Y. Ying, *Org. Lett.*, 2007, **9**, 3495–3498; (*b*) M. J. Iglesias, A. Prieto and M. C. Nicasio, *Adv. Synth. Catal.*, 2010, **352**, 1949–1954; (*c*) A. R. Martin, D. J. Nelson, S. Meiries, A. M. Z. Slawin and S. P. Nolan, *Eur. J. Org. Chem.*, 2014, 3127–3131; (*d*) M. A. Rodríguez-Cruz, S. Hernández-Ortega, H. Valdés, E. Rufino-Felipe and D. Morales-Morales, *J. Catal.*, 2020, **383**, 193–198.

12 It has been reported the use of monophosphine ligands in Pd-catalyzed C-S cross-coupling. See: J. Xu, R. L. Liu, C. S. Yeung and S. L. Buchwald, *ACS Catal.*, 2019, **9**, 6461–6466.

13 M. T. Martín, M. Marín, C. Maya, A. Prieto and M. C. Nicasio, *Chem. – Eur. J.*, 2021, **27**, 12320–12326.

14 J. E. Borowski, S. H. Newmann-Stonebraker and A. G. Doyle, *ACS Catal.*, 2023, **13**, 7966–7977.

15 (*a*) R. J. Rama, M. T. Martín, R. Peloso and M. C. Nicasio, *Adv. Organomet. Chem.*, 2020, **74**, 241; (*b*) V. M. Englert, P. W. Jolly and G. Wilke, *Angew. Chem.*, 1971, **83**, 84–85; (*c*) P. W. Jolly, K. Jonas, C. Krüger and Y.-H. Tsay, *J. Organomet. Chem.*, 1971, **33**, 109–122.

16 M. T. Martín, M. Marín, R. J. Rama, E. Álvarez, C. Maya, F. Molina and M. C. Nicasio, *Chem. Commun.*, 2021, **57**, 3083–3086.

17 (*a*) S. H. Newman-Stonebraker, J. Y. Wang, P. D. Jeffrey and A. G. Doyle, *J. Am. Chem. Soc.*, 2022, **144**, 19635–19648; (*b*) M. L. Clapson, D. J. Nelson and M. W. Drover, *ACS Org. Inorg. Au*, 2023, **3**, 217–222.

18 M. T. Martín, C. Maya, A. Galindo and M. C. Nicasio, *Adv. Synth. Catal.*, 2024, DOI: **10.1002/adsc.202400765**.

19 NiP_2 complexes reacted with electron-deficient alkenes such as styrene, maleic anhydride, dimethyl fumarate among others, but in all cases mixtures of bis-alkene and mono-alkene complexes were obtained that could not be separated.

20 P. B. Hitchcock, M. F. Lappert, C. MacBeath, F. P. E. Scott and N. J. W. Warhurst, *J. Organomet. Chem.*, 1997, **528**, 185–190.

21 (*a*) J. Wu, J. W. Faller, N. Hazari and T. J. Schmeier, *Organometallics*, 2012, **31**, 806–809; (*b*) S. Abe, T. Kosai, T. Limura and T. Iwamoto, *Eur. J. Inorg. Chem.*, 2020, 2651–2657; (*c*) M. Muhr, J. Hornung, J. Weßing, C. Jandl, C. Gemel and R. A. Fischer, *Inorg. Chem.*, 2020, **59**, 5086–5092.

22 A bent P–Pd–P angle was found in $[Pd(PCy_3)_2]$: E. Dinjus and W. Leitner, *Appl. Organomet. Chem.*, 1995, **43**, 50.

23 (*a*) W. J. Van Zeist and F. M. Bickelhaupt, *Dalton Trans.*, 2011, **40**, 3028–3038; (*b*) L. P. Wolters and M. Bickelhaupt, *ChemistryOpen*, 2013, **2**, 106; (*c*) F. Hering, J. Nitsch, U. Paul, A. Steffen, F. M. Bickelhaupt and U. Radius, *Chem. Sci.*, 2015, **6**, 1426–1432.

24 (*a*) P. H. Gehrtz, V. Geiger, T. Schmidt, L. Sršan and I. Fleischer, *Org. Lett.*, 2019, **21**, 50–55; (*b*) R. M. Oechsner, J. P. Wagner and I. Fleischer, *ACS Catal.*, 2022, **12**, 2233–2243.

25 L. Ortega-Moreno, M. Fernández-Espada, J. J. Moreno, C. Navarro-Gilabert, J. Campos, S. Conejero, J. López-

Serrano, C. Maya, R. Peloso and E. Carmona, *Polyhedron*, 2016, **116**, 170–181.

26 (*a*) M. Marín, J. J. Moreno, C. Navarro-Gilabert, E. Álvarez, C. Maya, R. Peloso, M. C. Nicasio and E. Carmona, *Chem. – Eur. J.*, 2019, **25**, 260–272; (*b*) M. Marín, J. J. Moreno, M. M. Alcaide, C. Maya, E. Álvarez, J. López-Serrano, J. Campos, M. C. Nicasio and E. Carmona, *J. Organomet. Chem.*, 2019, **896**, 120–128.

27 M. M. Colqhoun, J. Holton, D. J. Thompson and M. V. Twiggs, in *New Pathways for Organic Synthesis. Practical Applications of Transition Metals*, Plenum Press, New York, 1984.

28 D. J. Becke, *Chem. Phys.*, 1993, **98**, 5648–5652.

29 L. W. Yang and R. G. Parr, *Phys. Rev. B:Condens. Matter Mater. Phys.*, 1988, **37**, 785–789.

30 P. J. Hay and W. R. Wadt, *J. Chem. Phys.*, 1985, **82**, 299–310.

31 M. Cossi, N. Rega, G. Scalmani and V. Barone, *J. Comput. Chem.*, 2003, **24**, 669–681.

32 M. J. Frisch, G. W. Trucks, H. B. Schlegel, G. E. Scuseria, M. A. Robb, J. R. Cheeseman, G. Scalmani, V. Barone, G. A. Petersson, H. Nakatsuji, X. Li, M. Caricato, A. Marenich, J. Bloino, B. G. Janesko, R. Gomperts, B. Mennucci, H. P. Hratchian, J. V. Ortiz, A. F. Izmaylov, J. L. Sonnenberg, D. Williams-Young, F. Ding, F. Lipparini, F. Egidi, J. Goings, B. Peng, A. Petrone, T. Henderson, D. Ranasinghe, V. G. Zakrzewski, J. Gao, N. Rega, G. Zheng, W. Liang, M. Hada, M. Ehara, K. Toyota, R. Fukuda, J. Hasegawa, M. Ishida, T. Nakajima, Y. Honda, O. Kitao, H. Nakai, T. Vreven, K. Throssell, J. A. Montgomery Jr., J. E. Peralta, F. Ogliaro, M. Bearpark, J. J. Heyd, E. Brothers, K. N. Kudin, V. N. Staroverov, T. Keith, R. Kobayashi, J. Normand, K. Raghavachari, A. Rendell, J. C. Burant, S. S. Iyengar, J. Tomasi, M. Cossi, J. M. Millam, M. Klene, C. Adamo, R. Cammi, J. W. Ochterski, R. L. Martin, K. Morokuma, O. Farkas, J. B. Foresman and D. J. Fox, *Gaussian 09, Revision B.01*, Gaussian, Inc., Wallingford, CT, 2016.